Growth of sp-sp^2 nanostructures in a carbon plasma

Yasutaka Yamaguchi*
Department of Mechanical Engineering, Osaka University, 2-1 Yamadaoka, Suita, Osaka 565-0871, Japan

Luciano Colombo
Dipartimento di Fisica, Università di Cagliari and SLACS (INFM-CNR) Cittadella Universitaria, I-09042 Monserrato, Cagliari, Italy

Paolo Piseri, Luca Ravagnan, and Paolo Milani
Dipartimento di Fisica and CIMAINA, Università di Milano, Via Celoria 16, I-20133 Milano, Italy
(Received 9 July 2007; published 31 October 2007)

The growth of sp and sp^2 nanostructures in a carbon plasma is simulated by tight-binding molecular dynamics. The simulations are arranged so as to mimic the cluster formation conditions typical of a pulsed microplasma cluster source which is used to grow nanostructured sp-sp^2 carbon films [L. Ravagnan *et al.*, Phys. Rev. Lett. **98**, 216103 (2007)]. The formation of linear, ring, and fullerenelike objects in the carbon plasma is found to proceed through a very long multistep process. Therefore, tight-binding simulations of unprecedented duration have been performed by exploiting the disconnected topology of the simulated carbon plasma which made it possible to implement a computationally efficient divide-and-diagonalize procedure. Present simulations prove that topologically different structures can be formed in experiments, depending on the plasma temperature and density. A thorough characterization of the observed structures as well as their evolution (caused both by thermal annealing and by cluster ripening) is provided.

DOI: 10.1103/PhysRevB.76.134119 PACS number(s): 81.05.Tp, 61.43.Bn, 61.48.+c, 36.40.−c

I. INTRODUCTION

Spectroscopic and mass spectrometric investigations on the growth of fullerenes and nanotubes from a carbon plasma showed that small sp linear carbon clusters can be considered as metastable species evolving through cluster-cluster collisions and coalescence to form sp^2 cagelike nanoparticles.[1–4] Numerical simulations showed that small carbon chains are stable in high-temperature carbon plasma, while sp^2 hybridization becomes energetically favored and sp chains rearrange to form graphitic networks, as the number of atoms per chain increases.[5–8] The critical mass for sp-sp^2 conversion seems to depend on the thermodynamic conditions and, in any case, it should not exceed few tens of atoms.

On the other hand, an increasing number of experimental evidences show that sp-sp^2 hybridized carbon-based systems can be produced.[9,10] Recently, it has been reported that sp-sp^2 amorphous carbon films are obtained by depositing carbon clusters produced by a pulsed microplasma source.[11] Nanotubes encaging sp chains have also been observed.[12,13] Although preliminary theoretical reports provided support to the experimental findings,[14,15] a general understanding of the mechanisms underlying the growth and stability of clusters in which linear and planar structures coexist is still lacking, since the coexistence of both sp and sp^2 in the solid state seems contradictory to the energetic disadvantage of sp species against sp^2 formation.

This discrepancy can be understood by considering that spectroscopic characterization of carbon cluster and nanotube formation has been performed mainly on systems produced by laser vaporization of solid targets,[1,16,17] where carbon nanoparticles result from the condensation of a high-density, high-temperature plasma plume. The presence of a background gas can favor the thermalization of the hot vapor expanding at high velocity and driving the formation of metastable complexes.[18,19] The temperature during cluster growth upon laser ablation is in a range between 2500 and 4000 K lasting over a time scale of milliseconds, thus the cluster is subject to a substantial thermal annealing. We remark that this is the typical temperature range explored by numerical simulations of fullerene and carbon cluster formation.[20] Thermal annealing has been identified as a fundamental ingredient to transform sp structures into fullerenes and nanotubes as well as the driving mechanism through which disordered carbon clusters rearrange into ordered structures, consequently showing only even-numbered clusters typically for C_n $(n>30)$.[21]

Carbon cluster can also be produced by using a cluster source based on the plasma sputtering [pulsed microplasma cluster source (PMCS)] of a carbon target and the subsequent condensation of the sputtered species in an inert gas atmosphere,[22,23] where even- and odd-numbered large particles are produced with sp chains coexisting with sp^2 networks.[14] The working principle of a PMCS is the ablation of a target electrode by means of a spatially confined plasma discharge. The vaporized species are quenched by a pulsed helium beam and condense into clusters, transferring a reduced amount of energy to the extracted atoms and the background gas compared to laser vaporization. The condensation regime is similar to a gas aggregation source without interaction with a hot plasma plume. Moreover, in the PMCS, the temperature of the buffer gas during the cluster residence prior to extraction is in a range of 100–300 K so that no annealing takes place even for residence times of milliseconds.[23,24]

The key difference between PMCS and cluster ablation is the thermal annealing of the clusters during their residence in the source. The linear carbon sp chains with few tens of atoms transform into energetically favored well-ordered sp^2 network as the number of component atoms increases

through sufficient thermal annealing at high temperature in the laser vaporization technique. Meanwhile, the sp to sp^2 conversion is less favored in the PMCS technique free from thermal annealing, and metastable sp structures can be obtained even at room temperature, opening a potential for the investigation of sp carbon chains as an accessible new ingredient.

The isothermal growth of carbon cluster starting from gas-phase isolated carbon clusters was indeed simulated by using the molecular dynamics (MD) method with empirical classical potential.[25] The temperature effect on the structure was also investigated. The microcanonical simulations of the reaction path starting from sp-rich nested carbon layer were also carried out by using the same scheme as well.[26] In this simulation, the carbon layer self-annealed via a graphitic monolayer into a conjunct array of amorphouslike particles with a dimension about 10 nm, showing again that the temperature and annealing effects played an important role on the binding morphology of resulting structure.

Although the classical-MD scheme based on the empirical bond-order potential proposed by Brenner[27] is a useful tool which enables a long time-scale simulation with up to millions of atoms, the properties of sp-based structures are not well reproduced because the only chainlike compound adopted in the energy fitting is acetylene, and it is considered that the sp-sp^2 transition is rather biased. In addition, even a perfect sp^2 network without dangling bonds does not reject a further addition of small clusters, and that results in an unstoppable growth of the cluster even after the formation of a hollow caged fullerenelike network due to this "too sticky" interaction.[25]

Alternatively, in this paper, we carry out tight-binding molecular dynamics (TBMD), which represents a feasible possibility between the expensive *ab initio* and empirical interaction schemes. As described in Ref. 28 in detail, the most remarkable feature is that the TBMD scheme has both the feasible accuracy needed to describe systems with complex chemical bonding and a reduced computational workload suitable for comparatively large-scale simulations. The authors have also undertaken TBMD simulations of the growth of carbon structure under a high-density condition as well, where the isothermal aggregation starting from isolated 90 C_2 dimers (180 carbon atoms in total) is simulated with *NVT* ensemble at a density of 43.8 atoms/nm^3, i.e., 0.876 g/cm^3 corresponding to a density below a solid fullerite but above a vaporized graphite experimentally observed in laser ablation.[29] The carbon aggregate resulted in a final morphology of schwarzites with sp^2 network in a rather short time around 25 ps even at a high temperature of 3500 K. Further investigation on the high-density annealing is also carried out including the comparison of the Raman spectra of structures with experimental results.[15] A similar approach dealing with the formation of fullerenelike cage is also depicted in Ref. 20 using more precise density functional based tight-binding model, again showing the key role of sp chain which cannot be expressed through the classical approach.

In this study, a series of numerical simulations of the growth of carbon clusters under various temperatures and densities are performed using the TBMD scheme in order to investigate those effects on the morphology of the final product, while cooling of a hot cluster in buffer-gas atmosphere is preliminarily simulated using the classical-MD scheme as well to examine the time scale of the collisional dump of the kinetic energy.

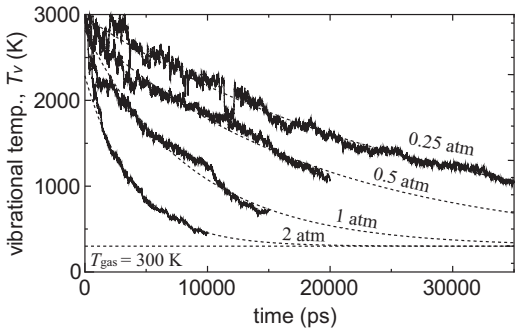

FIG. 1. Temperature decay of a single hot C_{20} cluster with an initial vibrational temperature T_v of 3000 K embedded in a helium buffer-gas atmosphere controlled at a constant temperature T_{gas}. Simulation here is carried out using classical empirical potential.

II. METHOD

As discussed above, the present simulation protocol is addressed to the PMCS experimental conditions. Accordingly, we need at first to focus on the key experimental features. We begin by observing that the clustering from gas-phase atomic carbon is surely an exothermic reaction, and that the reaction heat should be anyhow dissipated in order to ignite the growth process. In real experiments, the carbon clusters are cooled basically through the collision with the surrounding cold inert buffer gas (e.g., helium, argon atoms). Therefore, a computer-based simulation must incorporate such a feature.

In order to evaluate the cooling effect through collisions with buffer-gas atoms, a single C_{20} cluster with an initial vibrational temperature of 3000 K is put in a periodically repeated cubic cell with fixed $(40\ nm)^3$ volume, also containing helium atoms acting as a surrounding gas. The temperature of the buffer gas is controlled at 300 K by velocity scaling, while its pressure is set from 0.25 to 2 atm by changing the number of helium atoms. The interaction among carbon atoms is modeled by the Brenner empirical potential,[27] whereas the Lennard-Jones potential is applied for C-He and He-He interactions. This simulation is only targeted to evaluate the typical cooling rate.

The time evolution of the vibrational temperature T_v of C_{20} is shown in Fig. 1. As expected, the observed cooling rate through collisions becomes shorter as the helium pressure increases; nevertheless, the time scale of this process is as long as several nanoseconds at a pressure around 1 atm. In real experiments, the growth of sp and sp^2 structures can only proceed after cooling by which the energy due to the formation of interatomic bonds is dissipated. In other words, the real microstructure evolution of a carbon plasma interacting with a buffer gas does occur over a very long time period, not shorter than a few tens of nanoseconds. This is well beyond the possibility of a semiempirical quantum simula-

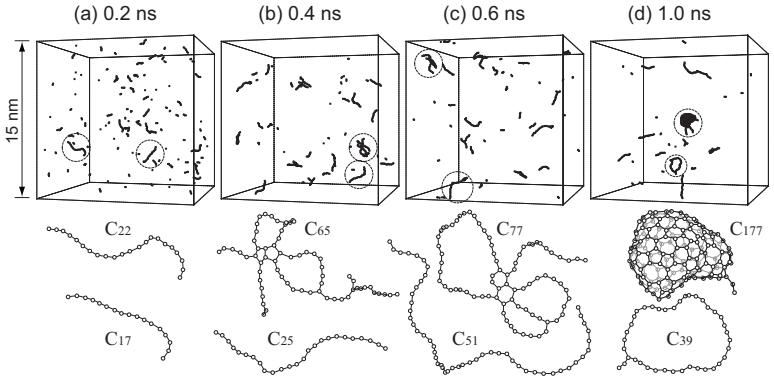

FIG. 2. An example of the simulation of the growth process of carbon clusters. Four hundred carbon atoms are randomly distributed in a $(15\ \text{nm})^3$ cubic cell as the initial condition, and the simulation is run under *NVT* ensemble at a control temperature $T_c=2000$ K. The whole system and two largest clusters at each time are displayed on the top and bottom, respectively, where every atom pair within a distance of 1.8 Å is considered to share a bond and is depicted with a solid line.

tion scheme, such as the TBMD one that we want to use in this work. Therefore, we decided not to simulate the coupling between the helium gas and the carbon dust. Rather, we omitted the buffer gas and we directly controlled the temperature of the carbon plasma. The cluster degrees of freedom are divided into translational, rotational, and vibrational ones and a corresponding temperature is defined for each of them. Such temperatures are independently set to a target value, according to the scheme discussed elsewhere.[25,30] This procedure allows us to skip the long, but inessential (as for bond formation), cooling process: TBMD simulations are therefore only addressed to the microstructure evolution of a given thermalized carbon plasma. The TBMD scheme adopted in this work is thoroughly described in Ref. 28, while the actual energy functional and the TB parametrization for carbon-carbon interactions are taken by Xu *et al.*[31] Such a TB representation has been proved to be successful in the simulation of quite a few different carbon-based systems.[32]

As for the simulation cell and initial conditions, 400 carbon atoms are placed with random velocities and random positions into a periodically repeated cubic cell. Several simulations at different thermodynamical conditions were carried out in order to survey the temperature and density effects on the resulting structure. In particular, five temperatures have been investigated, ranging from 100 to 3000 K; on the other hand, the cell volume varied from $(7\ \text{nm})^3$, to $(15\ \text{nm})^3$, and to $(32\ \text{nm})^3$, corresponding to 1.17, 0.119, and 0.0122 atoms/nm^3 density, respectively. Note that even the highest density of 1.17 atoms/nm^3 adopted here is still about 40 times lower than our previous simulations.[29] Atomic trajectories have been aged until the process of cluster formation is stabilized, i.e., when the actual cluster population formed so far was no longer evolving. The velocity Verlet algorithm was adopted to integrate the equation of motion with a time step $\Delta t=0.5$ fs.

As for the calculation of the Hellmann-Feynman contribution to the net force acting on each atom,[28] we needed to diagonalize the TB matrix of the whole system at every time step. We got a substantial reduction of the computational workload by exploiting the disconnected topology of the simulated system. As a matter of fact, the carbon dust is formed by several noninteracting subsystems (see Fig. 2, top), which are isolated from each other since their relative distance is well beyond the 2.6 Å cutoff of the adopted TB model. Accordingly, we solve independently the secular problem for each (small) TB matrix associated with each substructure the system was divided into. Of course, at each step of the simulation, the partitioning of the carbon dust into noninteracting subsystems was updated in order to take into account the microstructure evolution from the previous step of the TBMD loop. This operation, however, scales quadratically with the number N of atoms, rather than $O(N^3)$ as the brute-force diagonalization of one single large TB matrix. This reflects into a higher numerical efficiency, as proved in Table I where the boost factor provided by the above divide-and-diagonalize procedure is obtained by comparison with the elapsed time needed by a standard full-diagonalization approach.

III. RESULTS AND DISCUSSION

Figure 2 shows an example of the simulation of the growth process with 400 carbon atoms in a $(15\ \text{nm})^3$ cubic cell controlled at 2000 K. The whole evolving system and two different growing clusters are shown versus time on the top and bottom panels, respectively. Every atom pair within a distance of 1.8 Å is considered to form a bond (depicted with a solid line). Note that this definition of the bond is independent of the cutoff length of the tight-binding interaction. Bottom panels in (a)–(d) show that either linear chains (with sp bonding) and tangled chains or rings can indeed form. Interestingly enough, sp^2-bonded pentagons can act as cross-links

TABLE I. Boost factors against full diagonalization for various systems.

No. of clusters	No. of clusters C_n $(n \geqslant 20)$	Largest cluster	Boost factor
106	0	C_{14}[a]	293
44	5	C_{38}[b]	105
19	6	C_{179}[c]	9.1

[a]Corresponds to the one shown for 3000 K, 0.0122 atom/nm^3 in Fig. 3.

[b]Corresponds to the one shown for 2000 K, 0.0122 atom/nm^3 in Fig. 3.

[c]Corresponds to the one shown for 2000 K, 0.119 atom/nm^3 in Fig. 3.

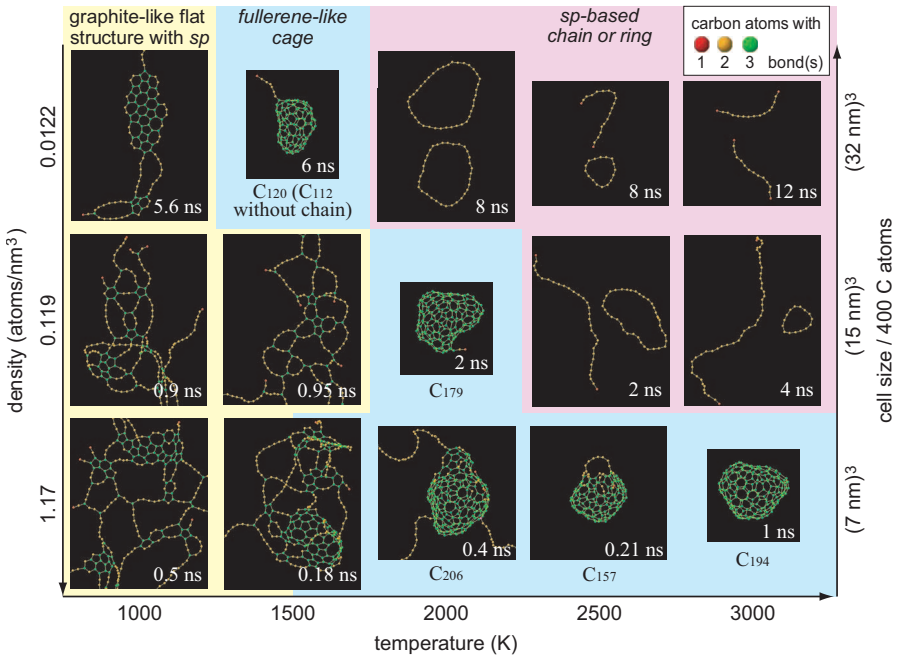

FIG. 3. (Color) Structures of clusters mapped on the temperature-density plane. The cell sizes adopted for simulations with 400 carbon atoms are also indicated on the right-hand side, and the largest clusters obtained under each condition are shown with the time. Corresponding movies are also available at our website (Ref. 33).

[see Fig. 2(b)] between neighboring structures. The sp^2 pentagons seen in Fig. 2(b) rearrange into hexagons bonded to chains partially linked so as to form polycyclic rings [see Fig. 2(c)]. Eventually, such polycyclic rings evolve to a hollow caged structure after about 1 ns [see Fig. 2(d)].

A synopsis of the different carbon structures produced by the present TBMD simulations is offered in Fig. 3, where the observed structures are mapped on a temperature-density plane. The actual cell size as well as the largest cluster obtained under each condition are also shown. The reported timing corresponds to the time after which a given structure is formed in the plasma for a given set of temperature and density. One-, two-, and threefold coordinated carbon atoms are colored as red, yellow, and green, respectively. Corresponding movies are also available at our website.[33] The resulting structures can be divided into three categories, namely, sp^2-bonded graphitelike flat structures, fullerenelike cages, and sp-bonded chains or rings. Their formation and evolution critically depend on temperature. At $T=1000$ K, the ripening of structures proceeds at first through the linking of sp chains. Then, linked chains partially graphitize to form sp^2 networks; present simulations, however, indicate that the graphitization process is definitely slower than the further extension of the sp links. In addition, the curvature leading to the wrapping of the whole two-dimensional network has never been observed at such a low temperature, so that no caged structure is expected even if the calculation is run further. At $T=1500$ K, the growth process is similar to the case of 1000 K, although closed cages may also be obtained at low density since graphitization seems to dominate with respect to further extension of sp linear chains. We should also mention that some fraction of sp-bonded atoms still remains, playing the role of defects among neighboring graphitelike fragments. By increasing the temperature up to $T=2000$ K, the morphology of the observed structures critically depends on the density: fullerenelike cages are very likely formed under high-density conditions, while sp chains or rings can only be observed for a lower density. Note that TBMD trajectories are aged for as long as 8 ns, i.e., until the system is fully saturated with no additional bond formation. The dominance of sp-bonded features is even more pronounced at temperatures as high as 2500 and 3000 K: in these conditions, the sp^2 network is only obtained at a very high density of 1.17 atoms/nm^3. It should also be mentioned that the sp^2-bonded schwarzites were obtained at $T=3500$ K for an even higher density of 43.8 atoms/nm^3 in our previous study.[29]

Let us now consider in more detail the microstructure evolution of a given cluster to work out the leading mechanisms driving the growth of carbon clusters. Figure 4 shows the history of the C_{174} cluster which is obtained by annealing at $T=2000$ K for 2 ns a plasma with 0.119 atom/nm^3 density. The cluster formation is represented against time in terms of either its growing size (left) or fraction of sp-bonded

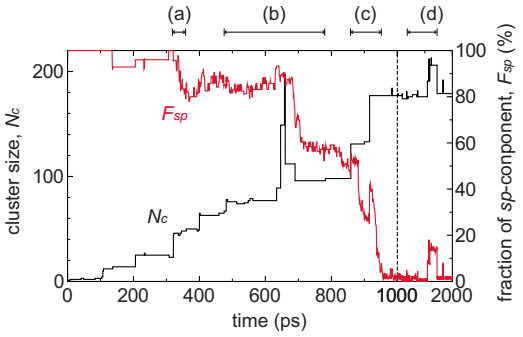

FIG. 4. (Color online) Growth history of the C_{174} cluster, which is obtained at 2 ns for the density and temperature of 0.119 atom/nm^3 and 2000 K, respectively, monitored as the cluster size and fraction of sp component to the cluster size to the time. The time range in the horizontal axis is enlarged until 1000 ps, and the detailed structural change during the time periods shown as (a)–(d) is illustrated in Figs. 5–8.

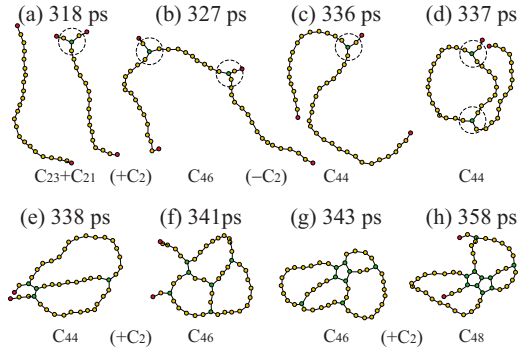

FIG. 5. (Color online) Formation of the neighboring pentagons shown as process (a) in Fig. 4. These initial stable nuclei generated through the collision of sp chains lead to the formation of the sp^2 network. Key structures of transient "trifurcates" are highlighted in dotted circles.

atoms (right). Here, sp-bonded carbons are defined as those atoms with two bonds colored in yellow in Fig. 3. The detailed structural changes during the observation time are illustrated in Figs. 5–8. As seen in Fig. 5(a), most of the smaller clusters take a chain or ring form; occasionally, we observe the formation of "trifurcates" which are highlighted in dotted circles in Figs. 5(a)–5(d). Trifurcates are rather unstable and, therefore, they have rather short lifetime. However, these unstable structures may promote through collisions with other species cross-linking which, in turn, can give rise to stable single or double neighboring pentagonal or hexagonal rings, as shown in Figs. 5(g) and 5(h). Once stable rings are formed, they work as seed of nucleation for larger graphitelike fragments: this is illustrated in Fig. 6. At this stage, the fraction of sp-bonded carbon atoms is still above 50%. During the growth process of the sp^2 fragments (which proceeds through the capture of chains from the surrounding plasma), the network often includes pentagonal rings which represent a coordination defect [see Fig. 7(b)]. The presence of pentagons has an important consequence for the topology, namely, they induce local curvature, leading to the creation

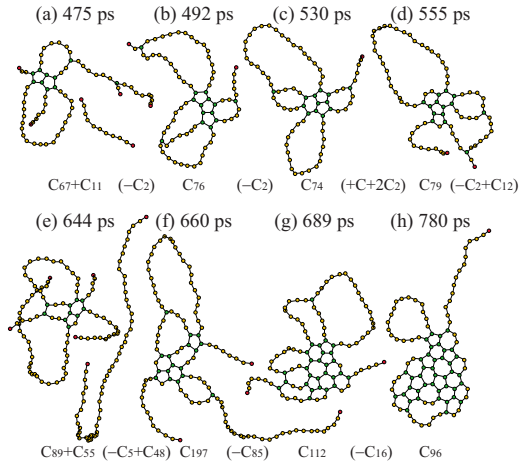

FIG. 6. (Color online) Extension of the sp^2 network around the neighboring pentagons shown as process (b) in Fig. 4.

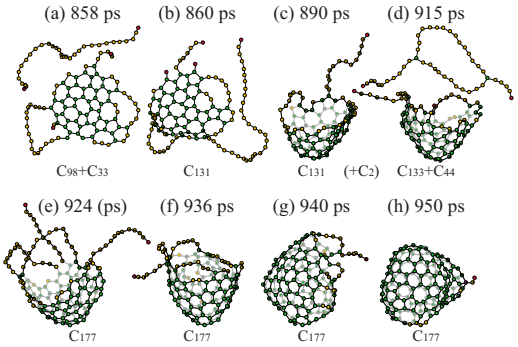

FIG. 7. (Color online) Formation of the fullerenelike cage shown as process (c) in Fig. 4. The closed cage is generated via the open cap through the wrapping of the open edge with additional sp chains.

of sp^2-bonded open-cap structures [see Figs. 7(c) and 7(d)]. This open end is then gradually filled by further addition of chains [as shown in Figs. 7(e)–7(g)] and, eventually, a closed cage is formed [Fig. 7(h)]. Short chains are likely not included in the close network and they remain attached outside, as a sort of tail. During this evolution, the fraction of sp-bonded carbon atoms decreases from about 50% to nearly 0%. After the closure, the cluster is rather stable against further growth. The more reactive parts of the outer surface are those ones characterized by a large value of the curvature radius: here, it is indeed possible to observe some interaction between the cluster and the surrounding plasma, as illustrated in Fig. 8, panels (d)–(f), where a linear chain sticks somewhere without modifying the cage. On the other hand, a smaller fragment like a C_2 dimer can be embedded into the cage, as shown in Fig. 8(c). The above rejection mechanism against further collision is very important since it works after the closure of a caged structure and prevents the cluster from endless growth. Present simulations suggest that the onset of such a mechanism occurs after relatively long times, when typical PMCS conditions are considered. This is a crucially important detail, marking an important difference between laser ablation technique and PMCS.

We finally want to readdress a twofold question: why sp^2 networks may exist only under high-density and/or low-temperature condition and why trifurcates seem to play an important role in the formation of a stable nucleation seeds. The lifetime of the trifurcates has been calculated as the average of their existing time in the temperature range between 2000 and 3400 K. The calculation was done for a system annealed for 8 ns at density of 0.0122 atom/nm^3 and tem-

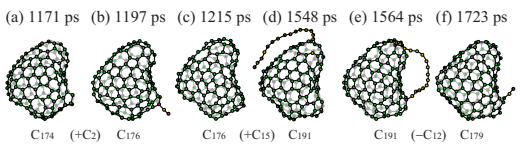

FIG. 8. (Color online) Structure of the closed cage in the time range shown as (d) in Fig. 4. The cluster is rather stable against the further growth due to additional collision except for the point with large curvature.

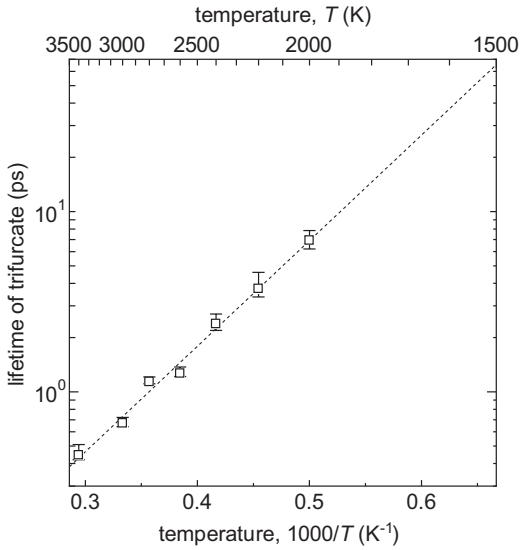

FIG. 9. Lifetime of the trifurcates (see Fig. 5) calculated as the average of their existing time for the temperatures ranging from 2000 and 3400 K. A system including ample number of chains and rings is adopted as the initial condition.

perature of 2000 K, respectively. This system was selected since it includes a large number of chains and rings. The logarithm of the estimated lifetime is plotted against the inverse of the temperature, as shown in Fig. 9. The key feature is that the lifetime of trifurcates is shorter than 10 ps at 2000 K. Under a low-density condition, the unstable trifurcates do not survive long enough to migrate and collide with other species so as to form a stable seed of nucleation. Rather, they redissociate into sp-bonded chains or rings. On the other hand, the trifurcates may be kept much longer than the collision interval at lower temperatures, and an unannealed network containing certain sp fraction can be formed.

IV. CONCLUDING REMARKS

The nanosecond-scale growth of carbon sp-sp^2 nanostructures starting from some hundreds of isolated gas-phase carbon atoms is simulated under various temperature and density conditions by using tight-binding molecular dynamics (TBMD) scheme in order to mimic as realistic as possible the PMCS experiment which can produce sp-rich nanostructures. The resulting structures can be categorized into three structures: sp-containing graphitelike flat structure, fullerenelike cage, and sp-based chain or ring, depending on the temperature and density. The metastable sp chains or rings preferably exist under high-temperature and low-density condition, while the sp-sp^2 transformation is highly promoted provided that these sp chains or rings may multiply collide with each other under high-density condition, and that leads to the production of the fullerenelike cage as the complete sp^2 network which basically consists of even number of carbon atoms and rejects further growth due to cluster collisions. Under low-temperature condition, on the other hand, the building blocks of the sp component remain with a certain fraction as the defect among the unannealed graphitized network which easily accepts further growth without showing the even-number rule. These results clearly show the specific property of the PMCS addressed as low-temperature low-density cluster generation technique in contrast to the laser ablation. The stability of the transient sp^2 trifurcate as the junction of sp chains plays a key role in the sp-sp^2 transformation.

ACKNOWLEDGMENTS

One of us (Y.Y.) thanks Jürgen Gspann at the University and Forschungszentrum Karlsruhe in Germany for useful discussions and support. This work was supported by the JSPS (Japan Society for the Promotion of Science) and Forschungszentrum Karlsruhe. Another author (L.C.) acknowledges support by MIUR under project PON-CyberSar (OR7).

*yamaguchi@mech.eng.osaka-u.ac.jp; http://www-gcom.mech.eng.osaka-u.ac.jp/~yamaguchi

[1] R. E. Smalley, Acc. Chem. Res. **25**, 98 (1992).
[2] N. S. Goroff, Acc. Chem. Res. **29**, 77 (1996).
[3] G. von Helden, M. T. Hsu, P. R. Kemper, and M. T. Bowers, J. Chem. Phys. **95**, 3835 (1991).
[4] *The Fullerenes*, edited by H. W. Kroto and D. R. M. Walton (Cambridge University Press, Cambridge, UK, 1993).
[5] K. S. Pitzer and E. Clementi, J. Am. Chem. Soc. **81**, 4477 (1959).
[6] J. R. Chelikowsky, Phys. Rev. Lett. **67**, 2970 (1991).
[7] R. O. Jones and G. Seifert, Phys. Rev. Lett. **79**, 443 (1997).
[8] S. Maruyama and Y. Yamaguchi, Chem. Phys. Lett. **286**, 343 (1998).
[9] L. Ravagnan, F. Siviero, C. Lenardi, P. Piseri, E. Barborini, P. Milani, C. S. Casari, A. Li Bassi, and C. E. Bottani, Phys. Rev. Lett. **89**, 285506 (2002).
[10] L. Ravagnan, G. Bongiorno, D. Bandiera, E. Salis, P. Piseri, P. Milani, C. Lenardi, M. Coreno, M. de Simone, and K. C. Prince, Carbon **44**, 1518 (2006).
[11] L. Ravagnan *et al.*, Phys. Rev. Lett. **98**, 216103 (2007).
[12] Z. Wang, X. Ke, Z. Zhu, F. Zhang, M. Ruan, and J. Yang., Phys. Rev. B **61**, R2472 (2000).
[13] X. Zhao, Y. Ando, Y. Liu, M. Jinno, and T. Suzuki, Phys. Rev. Lett. **90**, 187401 (2003).
[14] M. Bogana *et al.*, New J. Phys. **7**, 81 (2005).
[15] M. Bogana and L. Colombo, Appl. Phys. A: Mater. Sci. Process. **86**, 275 (2007).
[16] Y. Kato, T. Wakabayashi, and T. Momose, Chem. Phys. Lett. **386**, 279 (2004).
[17] S. Arepalli and C. D. Scott, Chem. Phys. Lett. **302**, 139 (1999).
[18] A. A. Puretzky, D. B. Geohegan, X. Fan, and S. J. Pennycook, Appl. Phys. Lett. **76**, 182 (2000).
[19] P. Milani and W. A. de Heer, Phys. Rev. B **44**, 8346 (1991).
[20] S. Irle, G. Zheng, Z. Wang, and K. Morokuma, J. Phys. Chem. B

110, 14531 (2006).
[21] J. M. Hunter, J. L. Fye, E. J. Roskamp, and M. F. Jarrold, J. Phys. Chem. **98**, 1810 (1994).
[22] E. Barborini, P. Piseri, and P. Milani, J. Phys. D **32**, L105 (1999).
[23] H. Vahedi Tafreshi, P. Piseri, G. Benedek, and P. Milani, J. Nanosci. Nanotechnol. **6**, 1140 (2006).
[24] K. Wegner, P. Piseri, H. Vahedi Tafreshi, and P. Milani, J. Phys. D **39**, R439 (2006).
[25] Y. Yamaguchi and S. Maruyama, Chem. Phys. Lett. **286**, 336 (1998).
[26] Y. Yamaguchi and T. Wakabayashi, Chem. Phys. Lett. **388**, 436 (2004).
[27] D. W. Brenner, Phys. Rev. B **42**, 9458 (1990).
[28] L. Colombo, Riv. Nuovo Cimento **28**, 1 (2005).
[29] S. Spadoni, L. Colombo, P. Milani, and G. Benedek, Europhys. Lett. **39**, 269 (1997).
[30] H. J. C. Berendsen, J. P. M. Postma, W. F. van Gunsteren, A. DiNola, and J. R. Haak, J. Chem. Phys. **81**, 3684 (1984).
[31] C. H. Xu, C. Z. Wang, C. T. Chan, and K. M. Ho, J. Phys.: Condens. Matter **4**, 6047 (1992).
[32] G. Galli, Comput. Mater. Sci. **12**, 242 (1998).
[33] Y. Yamaguchi, http://www-gcom.mech.eng.osaka-u.ac.jp/~yamaguchi/tbmd/index.html